Ballistic transport and scarring effects in coupled quantum dots

R. Akis and D. K. Ferry
Center for Solid State Electronics Research, and Center for Systems Science and Engineering, Arizona State University, Tempe, Arizona 85287-5706
(Received 12 August 1998)

We have performed numerical simulations of coupled, *open* quantum dots, connected by contacts supporting a number of modes. In single dots, the *resonant* wave functions can be *scarred* by classical periodic orbits. Coupling between dots allows for the two-dimensional analog of molecular states. With these molecular states, we find that the wave functions can be scarred by orbits that are clearly shared *between* dots. In a finite chain of dots, we find that the formation of energy bands and gaps can be a by-product of complicated scarred states involving orbits that can extend over many dots. These orbits appear to be variations of those that contribute to the atomic and molecular states. [S0163-1829(99)04311-8]

I. INTRODUCTION

Scarring is an effect whereby the quantum-mechanical wave function in a cavity has its amplitude maximized along the path of a periodic orbit that one would find in a corresponding classical billiard system with the same geometry. Seminal work in this area was performed by Heller and co-workers,[1–3] whose numerical calculations showed that the highly excited states of the Bunimovich stadium (which is classically chaotic) were scarred by unstable periodic orbits. The scarring effect has been found in other chaotic cavity systems, a noteworthy example being the Sinai billiard, which consists of a square or rectangular cavity with a circular diffuser in the center. In this case, the scarring has actually been observed experimentally in microwave cavities.[4–6] While the focus has been on chaotic systems, it has been shown that scarring can be a property of regular structures as well.[7] Scarring has also been observed in numerical simulations of *open* quantum cavities or dots. Specifically, scars have been found to correspond to *resonances* in the magnetoconductance in open square,[8] stadium,[9] and Sinai billiard[10,11] quantum dots connected to outside reservoirs by quantum point contacts (QPC's), which allowed several propagating modes. In these simulations, certain scarred states were found to recur periodically in magnetic field. The periodicities obtained have been found to match well those observed in experimental magnetoconductance fluctuations of such dots,[8,12] yielding circumstantial evidence that the periodicity of the fluctuations can be associated with the periodic orbits underlying the scars.

Recently, there has been much interest in the physics of coupled quantum dots. Single dots can be considered analogous to ''artificial atoms'' if the energy levels can be resolved.[13] Thus, fabricating multiple quantum dots that are coupled together by QPC's provides a way of creating ''artificial molecules.'' Most of the work has focused on the situation where the coupled dots have been connected to external reservoirs by QPC's that are in the tunneling regime so that the physics is dominated by Coulomb blockade effects.[14] However, one should still expect the transport to be dominated by the resolvable spectrum even in ''open'' dots (QPC's allowing several modes) provided that the mean free path and phase coherence length are larger than any characteristic dot dimension.[15,16] Provided that the number of propagating modes is not too great, a collimation effect is produced by the QPC's that can cause the selective excitation of particular dot eigenstates.[8,17] This selection of states is believed to be due to the fact that the collimation effect allows only certain orbits to participate.[8] The scarring effect seen in resonant states in open dots serves as evidence for this claim.

In this paper, we extend our previous work[8–10,12] by examining coupled dots that are in the open regime. As was the case in single dots, we find that scarred states can play an important role in ballistic transport. When two dots are coupled, we find that conductance resonances that correspond to ''molecular'' states can be scarred by classical orbits that are clearly shared between dots. Simulating finite chains of dots, we obtain the expected superlattice behavior (the formation of bands and gaps), but find that this behavior can occur as a result of the formation of complicated scarred states that involve orbits that can extend over many dots. Significantly, these orbits appear to be more complicated variations of those that contribute to the single and double dot states.

The paper is organized as follows. In Sec. II, our method of calculation is briefly described. In Sec. III, we consider the case of two coupled dots. In Sec. IV, the focus is shifted to superlattices of coupled dots. Conclusions are drawn in Sec. V.

II. METHOD OF CALCULATION

In this section, we briefly summarize our method of calculation. For full mathematical details, we refer the reader to.[18] For our simulations, the general situation is one in which ideal quantum wires, which extend outward to $\pm\infty$, are connected to the dot system. When a magnetic field is applied, it is normal to the plane of this system. We solve this quantum-mechanical problem on a discrete lattice using an iterative matrix method that is a numerically stabilized variant of the transfer matrix approach. The discretized Schrödinger equation, keeping terms up to first order in the approximation of the derivative, has the form

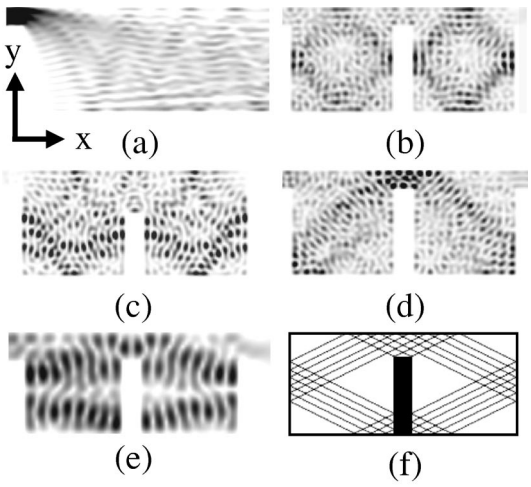

FIG. 1. In (a)–(e), $|\psi(x,y)|$ vs x and y is plotted, with darker shading corresponding to higher amplitude, showing scars for the situations described in the text. A classical periodic orbit is plotted in (f).

$$(E_F-\mathbf{H}_j)\psi_j+\mathbf{H}_{j,j-1}\psi_{j-1}+\mathbf{H}_{j,j+1}\psi_{j+1}=0, \qquad (1)$$

where ψ_j is a M-dimensional vector containing the amplitudes of the jth slice. This problem is solved on a square lattice of lattice constant a with the wires extending M lattice sites across in the y direction. The region of interest [for example, the QPC and open ended cavity shown in Fig. 1(a)] is broken down into a series of slices along the x direction. In this equation, the $\mathbf{H}_j$ matrices represent Hamiltonians for individual slices and the matrices $\mathbf{H}_{j,j-1}$ and $\mathbf{H}_{j,j+1}$ give the interslice coupling. By approximating the derivative, the kinetic energy terms of Schrödinger's equation get mapped onto a tight-binding model with $t=-\hbar^2/2m^*a^2$ representing nearest-neighbor hopping. The potential V at site i,j simply adds to the on-site energies, which appear along the diagonal of the $\mathbf{H}_j$ matrices. Transfer matrices based on Eq. (1) can then be derived, which allow translation across the system to obtain the transmission coefficients, and which, in turn, enter the Landauer-Büttiker formula to give the conductance. The instability problems inherent in the transfer matrix approach due to exponentially growing and decaying contributions of evanescent modes are overcome by some clever matrix manipulations.[18] Rather than just multiplying transfer matrices together, the scheme is turned into an iterative procedure that does not allow the eigenvalues to diverge. Once the calculation is complete, the wave function can be reconstructed by a backsubstitution scheme. In order to approximate well the continuous system, the lattice spacing a must be small compared to the Fermi wavelength λ_F, typically on the order of $\sim 0.1\lambda_F$ or smaller.

Figure 1(a) illustrates beam collimation effect mentioned in the introduction, which we believe plays an important role in determining which orbits participate in the transport. Here $|\psi(x,y)|$ versus x and y plotted for a QPC 0.06 μm wide, supporting three propagating modes given a Fermi energy of $E=16$ meV. The QPC exits into a 0.3-μm-wide cavity. With the quantization of the transverse velocities in the QPC, the electrons exist at well-defined angles (note that the beam quite visibly splits into the three modes) and this combined with upper boundary reflection creates the downward collimation. While we for the most part present results in the quantum regime, it should be noted that the role of beam collimation as a selector of orbits has been verified in purely *classical* simulations of an open square cavity at *finite magnetic field*.[8] By an examination of Poincaré plots, it was found that only a comparatively small region of phase space was visited if the electrons were injected via a collimated beam at a particular angle with some small spread.

II. TWO DOTS IN SERIES

Classically, *closed* square cavities have been shown to yield a mixture of regular and chaotic behavior with finite B.[19] As for the periodic scarring effects, diamond scars were seen to recur in single open dots nominally square in shape.[8,12] In Fig. 1(b), we show an example for two coupled dots. Each dot is a 0.3 μm square and the three fingers that define the two dots are each 0.05 μm wide [E and the QPC's are the same as in (a)]. A perpendicular magnetic field of $B=0.280$ T has been applied (the cyclotron radius is $r_{\rm cyc}\sim 0.4\,\mu$m). In each dot, $|\psi(x,y)|$ is scarred by a classical periodic orbit in the form a diamond. In a single dot, these wave functions correspond to resonances[8] and so can be considered analogous to atomic states.

At first glance, this picture seems odd as the orbit reflected by the scar does not *appear* connected to either lead. However, it is important to realize as these correspond to *resonant* states, the electrons can stay in the dot for a rather long time. In a calculation where inelastic scattering was introduced to limit the phase coherence length, it was estimated that the electrons would have to make on the order of 20 circuits along the diamond orbit in order to build to sufficient amplitude to form the scar.[20] Since the electrons enter and exit the dot system only once, the quantum-mechanical amplitude associated with those paths is dwarfed by comparison, as are the contributions made by any shorter orbits that may be allowed in the dot. The conclusion that scars correspond to long-lived states is supported by the dwell time analysis of Zozoulenko *et al.*[21] In semiclassical calculations of conductance, the orbits that are usually singled out are short and show a clear and relatively simple connection with the input and output lead (see, for example, Wirtz, Tang, and Bergdorfer[22]). However, examining resonant states is typically not done in these calculations, as the very long *quasiperiodic* orbits (recall the electrons are confined for a finite time) which lead to the resonant behavior are not included. This is because a cutoff length (expressed in terms of the number of bounces an orbit makes, 15 being a typical number) is imposed in order to allow the calculations to finish in a reasonable amount of time.[23] This is not an issue with our fully quantum-mechanical transport calculations. In fact, in a system such as ours where the quantum dots are well defined one can begin making direct comparisons with the semiclassical theory of *closed* systems, where the density of states (DOS) is determined by weighted summations over truly periodic orbits.[24] Indeed, examining the conductance G in open quantum dots as a function of both energy E and field B, it has been found that the resulting three-dimensional function is prominently striated by lines of resonances.[25,26] These resonance lines tend to coincide to points where one finds scarred wave functions such as the diamond shown

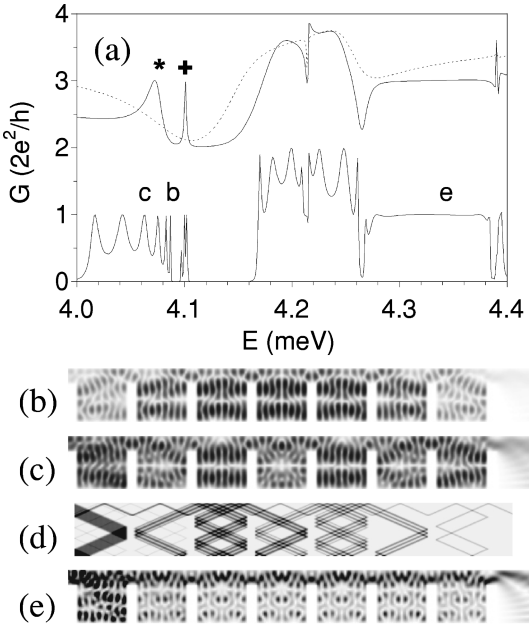

FIG. 2. (a) G vs E plotted for one (upper dashed curve), two (upper solid curve), and seven quantum dots (lower solid curve). The two upper curves have been offset by a factor of $G=2e^2/h$. (b), (c), and (e) are the wave functions that correspond to the indicated features in (a). A classical distribution function is plotted in (d).

here.[25] *They also tend to coincide to lines found in the actual spectrum of the closed dot.*[26] As one might expect, the match between $G(E,B)$ and the closed dot spectrum is not exact since the openness of the dot broadens the energy levels, but the basic pattern is the same.[26] An important point is that the broadening is *not uniform*. In particular, which closed dot states survive to yield resonance lines in the conductance of the open system has been found to be highly dependent on not only the width of QPC openings, but on their position as well.[25] For example, if the QPC's are shifted down to the center of the dot, the diamond orbit is no longer allowed. In this case, the resonance lines corresponding to states scarred by this orbit vanish.[25] This result serves as yet another confirmation of the fact that the QPC's act as a selector of particular orbits.

With regard to scarring in closed systems, a semiclassical ''scarring'' formula has also been derived in a manner similar to that of the DOS formula.[27] It relates the wave-function amplitude squared integrated over a range of energy to a weighted summation over periodic orbits. As a result of the nature of the weighting, the more stable orbits contribute more strongly than the others and as such are reflected in the wave functions. This is the origin of the scarring effect. While this semiclassical formula requires an integration over energy, it is consistent with the results that show individual eigenstates being scarred. This is permitted provided that the energy level spacing is sufficiently large. The semiclassical formula for the DOS and scarring apply in the limit $h\rightarrow 0$. In the fully quantum-mechanical theory we employ, this is equivalent to requiring that the states that are examined be at high energy, so that a large number of nodes are present in the wave function [examining the ripples underlying the scars in Fig. 2(b), one can see about $\sim$18 antinodes along the x and y directions]. Indeed, a relatively large number of antinodes are required in order to resolve a scar. This is why we see scarring in our coupled dot results, while Li and Berggren,[28] who also examined what may be considered open, coupled quantum dots (actually a quantum wire with double stub side branches), did not. They only considered the very lowest part of the energy range and the first few resonant states. Among other things, they also examined the quantum-mechanical current flow and saw that the resonant states yielded vortices. With regards to this, we note that it can be dangerous to associate quantum-mechanical current flow lines with classical trajectories, particularly at low energy. For example, the lowest resonant state in a quantum wire with a cross branch has a single antinode trapped in the region where wire and branch intersect and is held in place by the sharp corners of the structure. The flow lines associated with the current vortex corresponding to such a state have *no* direct relationship to any classical orbit. We have found that a simple correspondence between current flow and a classical trajectory only occurs when the scarring of the resonant state is particularly obvious, such as the diamond scar shown here. In this case, current circulates around and along the diamond.

In Fig. 1(c) is what may be described as a ''molecular'' state. The QPC connecting the dots has been widened to 0.12 μm. Here it appears that a precession effect is occurring, with electrons roughly following the diamond, but then deviating from it, and eventually skipping into the adjacent dot. One can observe this sort of sharing effect even if the individual dots remain very well defined. Figure 1(d) corresponds to the same situation as 1(b), but now $B=0.042$ T ($r_{\rm cyc}\sim 2.6\,\mu$m). An inverted V-shaped scar clearly extends between the two dots. Given the collimation effects shown in Fig. 1(a), it is not difficult to understand why the classical orbit that scars this state is being favorably occupied, likely by the middle portion of the split beam in Fig. 1(a). For Fig. 1(e), we have set E to be 4.073 meV, the QPC's are 0.08 μm wide, supporting two propagating modes and $B=0$. Here a more complicated variation of the type of ''shared'' scar shown in Fig. 1(d) appears. With the change in conditions (lower energy, zero field, wider QPC's) the aim of the collimated beam has been significantly altered. Thus, as one might expect, a different orbit is reflected by the resonant state. An example of a classical orbit that is closely related to this scarred state is shown in Fig. 1(f). As one may imagine, there are a large number of periodic orbits that have this same basic form (they of course would involve greater or lesser numbers of bounces). As Heller, O'Connor, and Gehlen have noted,[3] because orbits tend to come in families (''cousins''), it can be difficult to make a one to one correspondence between a particular scarred state and a specific orbit. However, it is clear that one can at least make a correspondence to a family.

III. FINITE SUPERLATTICES OF DOTS

In Fig. 2(a), we plot conductance G versus energy E for one, two, and seven dots and use the dot configuration of Fig. 1(e). The upper solid curve is for two coupled dots and the resonance marked by the * corresponds to Fig. 1(e). This resonance as well as the one adjacent to it (marked +) do *not* occur in the upper dashed curve, which is for a single dot.

This is not surprising since the scars here require at least two dots to be established [the + resonance corresponds to an inverted-V pattern similar to Fig. 1(d)]. Importantly, the two dot and one dot curves still do share resonances in common, at ~4.21 and ~4.39 meV. There is some splitting of the resonances the two dot case due to the interdot coupling breaking the degeneracy of the single dot states. The middle solid curve corresponds to seven coupled dots and shows sets of resonances as well as flat plateaus. This is a more complicated variation of behavior previously noted for finite one-dimensional (1D) superlattices.[29,30] Specifically, if there is a resonance in transmission through a single 1D potential well, the N such wells coupled together will produce N peaks in transmission as a function of E. These peaks correspond to standing waves with different numbers of nodes trapped in the structure. As N is made infinite, these groups of peaks eventually correspond to energy bands, and the transmission minima separating them to band gaps. However, unlike the purely 1D case, there are two propagating modes in the QPC's here, so that there are there three quantized steps in conductance possible instead of just $G=0$ and $G=1$ (in units of $2e^2/h$). From the figure, one sees the groups of resonances peaking either at $G=1$ or $G=2$ and flat plateaus correspond to either $G=0$ or $G=1$. As in the 1D case, if we increase the number of dots in the structure, more resonances appear in each group and they eventually form ''quasiplateaus.'' A ''recovery of quantization'' similar to what is seen here was first noted by Leng and Lent[31] in a quantum wire with a relatively weak periodic modulation. Three of the features in the curve are labeled *b*, *c*, and *d*. Figure 2(b) is the wave function at *b* (a resonance at $E=4.087$ meV). The amplitude is maximized in the center and there is a standing wave with a single antinode trapped in the structure. Figure 2(c) corresponds to *c* (a resonance at $E=4.063$ meV), which occurs in the same finite band as Fig. 2(b). A more elaborate standing wave occurs, with several more antinodes. For comparison, Fig. 2(d) shows a *classical* distribution within an open seven dot structure. To generate this picture, we injected an angled beam of classical electrons into the left side of the structure, which is broken down into a grid. To determine the shading, we counted the number of times an electron passes through a grid element in its trip through the structure, with darker color for higher counts. Clearly evident are a series of interlocking orbits that are more complicated variations of the orbit in Fig. 1(f). Note, in particular, the presence of orbits that appear to be spread across three dots instead of two. These orbits form patterns similar to those evident in the wave functions shown above. Thus, we conclude that, in general, the standing waves are not just a simple linear combination of the original scarred states. They are in fact the quantum remnants of the type of multidot orbits shown in Fig. 2(d), obviously related to the original orbits, but clearly modified by the multidot structure. Figure 2(e) corresponds to the $G=1$ plateau labeled *e* ($E=4.35$ meV). Interestingly, this plateau appears to occur as the result of an underlying skipping orbit that bounces off the top edge of each finger [segments of such a trajectory can be seen in Fig. 2(d)]. However, in contrast to the quantum Hall effect, the skipping orbit present here occurs at *zero field* and is *not* related to any magnetic edge states. We find that these zero-field skipping orbits can occur in many different situations, particularly when $G=1$. Analogous zero-field skipping orbits have been observed in quantum-mechanical calculations performed on 2D antidot superlattices.[32] Different types of behavior leading to plateaus are discussed below.

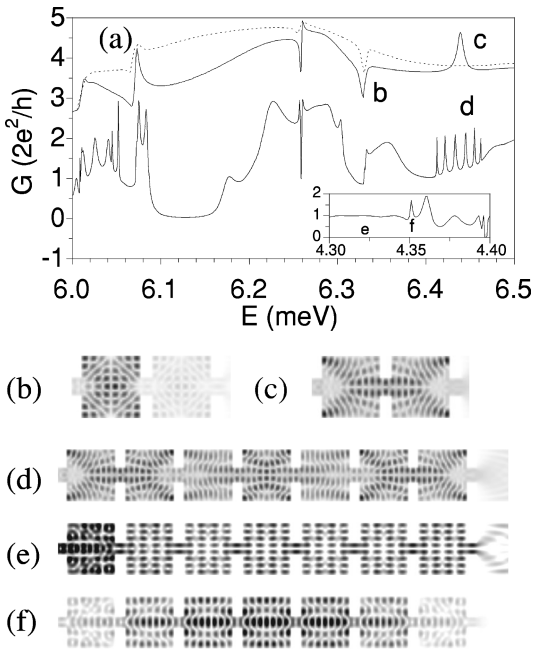

FIG. 3. (a) G vs E is plotted for one (upper dashed curve), two (upper solid curve), and seven quantum dots (lower solid curve). In this case, the QPC's have been moved to the centers of the dots. The two upper curves have been offset by a factor of $G=4e^2/h$. Inset: G vs E for the same seven dot structure, but with QPC's that have been narrowed. (b), (c), (d), (e), and (f) are the wave functions that correspond to the indicated features on (a).

In Fig. 3, we show an example with a different lead configuration. The dots are the same size as above, as are the widths of the fingers. The QPC openings in this case are 0.08 μm, wide enough to support three propagating modes for the given energy range. Here, the leads have now been shifted down to the center of each dot. In this case, the electrons exit the leads in a V-shaped jet. In Fig. 3(a), we plot conductance G versus energy E for one, two, and seven dots. Figures 3(b) and 3(c) show the resonant double dot wave functions corresponding to labels *b* ($E=6.329$ meV) and *c* ($E=6.45$ meV) in Fig. 3(a). Note that only a single resonance at *b* occurs in both the one and two dot curves. Examining the wave function at *b*, we see that the pattern in both dots reflects a pair of crossed rectangular orbits, tilted at an angle of 45°. As in Fig. 1(b), this is an example of two ''atomic'' states that are very weakly coupled together. Looking at the seven dot curve, there is a wide minimum where the resonance occurred in the one dot curve. Adjacent to this minimum are weak side resonances. The behavior here is reminiscent of that noted for quantum wires with single stub side branches.[33] In contrast to simple one-dimensional problem of potential barriers in series, which allows only for resonant transmission, it was found that the quasibound states in stubbed quantum wires could actually yield resonant reflections (for a simple qualitative explanation of this behavior see Ref. 34, for a review of the subject see Ref. 35 and references therein). In the case where several stubbed wire

sections are connected in series, it was found that these reflection resonances broadened into valleys due to the cumulative blocking effect of the resonant states trapped in the stubs.[36] Here a similar effect is apparent. While the pattern in each dot is the same, the amplitude in the second in Fig. 3(b) is much weaker than in the first. At the resonance labeled *c* ($E=6.435$ meV), the wave function shown in Fig. 3(c) yields yet another example of a ''molecular'' state, with two crossed rectangular orbits extending between the two dots (note that the resonance is absent in the one dot case). The occurrence of this resonant state is obviously facilitated by the position and collimation effect of the leads. In the seven dot curve, there are six resonances in this region of energy, each corresponding to different standing waves trapped in the structure. The one corresponding to $E=6.445$ meV is shown in Fig. 3(d). As with the previous example, the standing waves reflect more complicated variations of orbits apparent in the ''molecular'' state.

The inset of Fig. 3(a) shows G versus E for a seven dot, centered lead superlattice as well. In contrast to the previous example, the QPC openings have been narrowed to 0.06 μm, so that only two modes propagate over the given energy range. Note that, over this range, there is a $G=1$ plateau and several resonances. The wave function for the plateau is shown in Fig. 3(e) ($E=4.325$ meV). In contrast to Fig. 2(e), where a skipping trajectory was clearly reflected by the wave function, no trajectory pattern can be discerned. Indeed, the simple checkerboard patterns that are exhibited in the individual dots in the last six dots of the structure are what you would expect for many of the eigenstates of a *closed* square dot. The pattern evident in the first dot is similar to the bound state that you would see at resonance in a single dot near this energy. The wave function here is comparatively complicated, so it is difficult to picture what the orbit corresponding to this pattern might be. That said, it is clear that collimation has had a considerable effect on the formation of this state. Note the V-shaped jet exiting the final QPC (corresponding primarily to the second mode) and that the amplitude in the top and bottom parts of the first dot is concentrated in the right-hand side. A resonant wave function is shown in Fig. 3(f) ($E=4.351$ meV). Here is a standing wave with a single node. The amplitude in this case seems to be highly concentrated along the central axis of the dot. This concentration results in large part due to the first QPC mode, which exits with a small angle compared to the second mode. The effect here is superficially reminiscent of the ''channeling'' states found in 2D antidot superlattices.[32] In those Bloch states, the quantum-mechanical *current* is highly concentrated between rows of antidots and was found to flow almost exclusively along the positive x direction. Here, while the amplitude is somewhat concentrated, there is no unidirectional current flow. This is to be expected as it corresponds to a quasibound state. That said, it should be noted that the sort of skipping behavior shown in Fig. 2(e) for the top lead case is not disallowed in the centered lead case. What is required is the right combination of QPC opening and lattice spacing in order to aim the collimated beams exiting the QPC's correctly to yield the desired effect.

In Fig. 4, we now consider a Sinai billiard structure. The solid curve in Fig. 4(a) is the conductance for a seven-unit-cell chain. Here the QPC's have been pushed to the bottom

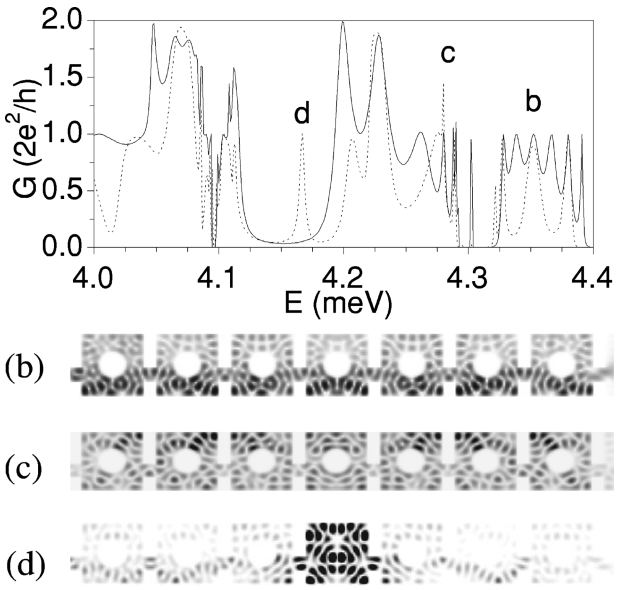

FIG. 4. (a) G vs E is plotted for a chain of seven Sinai billiard quantum dots (sold curve) and a Sinai billiard chain with a defect (dotted curve). Figures (b), (c), and (d) are the wave functions that correspond to the indicated features on (a).

half of each dot and a 0.07-μm radius antidot has been included in each. While the closed, classical Sinai billiard is chaotic for $B=0$, there is no qualitative difference between the behavior in chains of Sinai billiard structures and that of square dots. Figure 4(b) corresponds to the resonance labeled *b* in Fig. 4(a) ($E=4.35$ meV). Here we see a standing wave pattern involving scars trapped in the lower part of each dot. As with the square dot example, this wave does not involve a simple repetition of a single dot resonant state. Another resonant state is shown in Fig. 4(c) ($E=4.35$ meV). In this case, the resonant standing wave state has amplitude primarily trapped in the upper corners of the cavities. The dotted curve in Fig. 4(a) corresponds to a Sinai billiard chain with a defect (there is no antidot in the fourth dot). As one expects in a periodic system with a defect, a localized state arises in a band gap [labeled *d* in Fig. 4(a)]. This state, shown in Fig. 4(d), is dominated by a ''twist-tie'' scar trapped in the defect dot.

In Fig. 5, we now consider the effect of a magnetic field. Figure 5(a) shows G versus B for one, two, and eleven dots. As before, the dots are 0.3 μm square. Here $E=4$ meV and the QPC's allow three propagating modes. The one dot (dashed line) and two dot (dotted line) curves show one main resonance, but the 11 dot curve has several. Thus, as Leng and Lent found,[31] we see a build up of resonances with B as well as with E. The wave function corresponding to the resonance marked *b* ($B=0.259$ T) is shown in Fig. 5(b). Here we see a one antinode standing wave where the individual dots are scarred by diamond orbits similar to those shown in Fig. 1(b). A two antinode wave is shown in Fig. 5(c) ($B=0.251$ T). The standing waves in this case appear to be simply related to the single dot ''atomic'' states. Indeed, in the broad minimum before resonance *b*, there is the blocking behavior noted in the centered lead case. This is shown in Fig. 5(d), which corresponds to $B=0.251$ T. Note that the diamond pattern becomes fainter as we progress through the

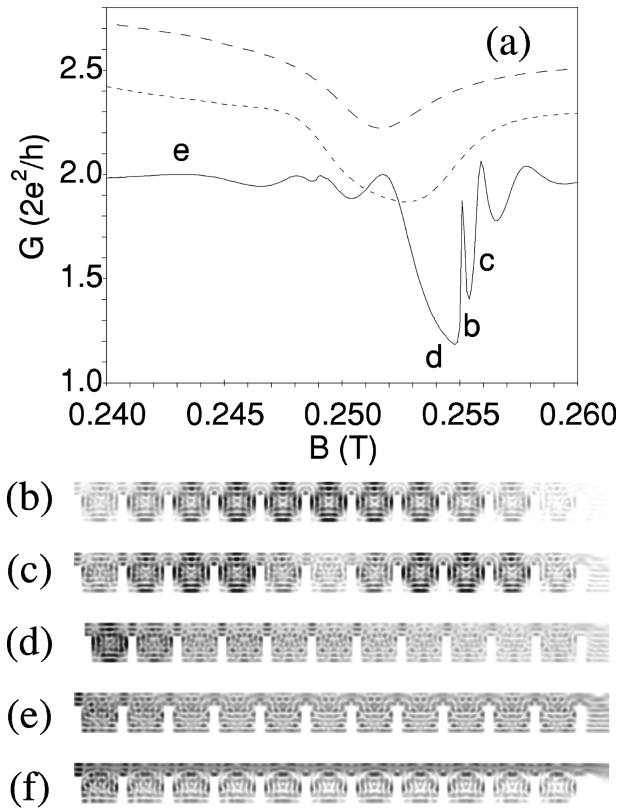

FIG. 5. (a) G vs B is plotted for a one dot (long dashed line), two dots (short dashed line) and 11 dots (solid line). Figures (b) through (f) are the wave functions that correspond to the indicated features on (a). Figure (f) is the 11 dot wave function for $B=-0.243\,\mathrm{T}$.

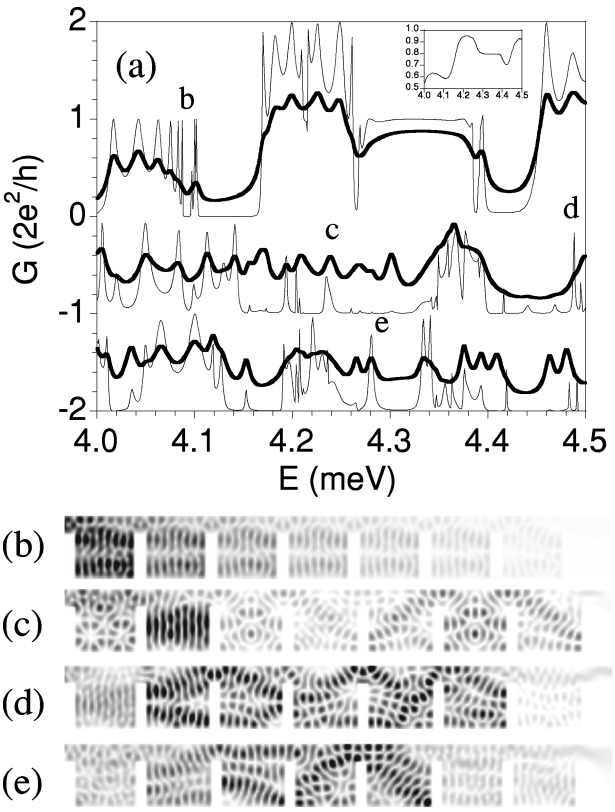

FIG. 6. (a) G vs E for the original seven dot chain for no phase breaking (upper thin line) and with phase breaking corresponding to $\tau_\phi=100\,\mathrm{ps}$ (upper thick line), a seven dot chain with disorder (middle thin line), disorder and phase breaking (middle thick line), a different disorder configuration (lower thin line) and that disorder configuration and phase breaking (lower thick line). The middle curves and bottom curves have been offset by factors of $G=-2e^2/h$ and $-4e^2/h$, respectively. Inset: the original seven dot chain, but with $\tau_\phi=100\,\mathrm{ps}$. Figures (b), (c), (d), and (e) are the wave functions that correspond to the indicated features on (a).

structure. The wave function [Fig. 5(e)] occurs on a plateau ($B=0.243\,\mathrm{T}$). In contrast to Fig. 2(e), which showed a skipping orbit, this plateau wave function shows what might be described as a series of partial diamonds in each dot. Thus, it appears that a more open variation of the orbit that leads to resonant states in the individual dots leads to this plateau. Note that, in contrast to the gradual decay shown in Fig. 5(d), the amplitude stays essentially constant throughout the entire structure. What happens when the sign of B is flipped ($B=-0.243\,\mathrm{T}$ here) is shown in Fig. 5(f). The sign flip yields the same conductance, as demanded by the Onsager-Casimer relations, but the dots in Figs. 5(d) and 5(e) clearly show significantly different variations of the diamond pattern [it is stronger in Fig. 5(e)]. Classically, this is understandable since the sign of B determines whether the trajectories are bent upward or downward via the Lorentz force [note the amplitude pile up at the top in Fig. 5(e)]. On the other hand, for the resonant states [Figs. 5(b) and 5(c)], the sign flip simply generates nearly identical wave functions, but a reversal in the direction of quantum-mechanical current circulating around each dot orbit. Importantly, as they correspond to resonances, it can be shown that states analogous to Figs. 5(b) and 5(c) occur in the *closed* 11 dot system. Needless to say, Figs. 5(e) and 5(f) have no analog in the closed system.

Are these effects robust to the phase breaking and disorder expected in a real system? Oscillations such as we have shown in the preceding figures here have been seen *experimentally* by Kouwenhoven *et al.*[37] in an actual superlattice of quantum dots. Since it was an experiment, additional effects such as rounding of the dot potentials by self-consistent electron effects and defects in periodicity were automatically included. However, those experiments were performed at a comparatively high field ($B=2\,\mathrm{T}$). The presence of such a field overcomes much of the backscattering that impurities would otherwise cause.[38] With regard to phase breaking, inelastic scattering can be introduced phenomenologically by adding an imaginary potential $V_{\mathrm{in}}=-i\hbar/(2\tau_\phi)$, where τ_ϕ is the inelastic scattering time.[39] Figure 6 shows what occurs for the seven dot structure considered in Fig. 2. The thin curve at the top of Fig. 6(a) is a reproduction of the seven dot curve from Fig. 2(a). The thick curve overlayed on top of it was generated using $\tau_\phi=100\,\mathrm{ps}$, comparable to values measured in real dots of this size[40] (the corresponding path length is $l_\phi=\nu_F\tau_\phi\sim 7\,\mu\mathrm{m}$). The broader resonances survive while the sharper ones vanish, showing up as points of inflection, or merge with adjacent resonances. As with resonant tunneling, the width of the peak of a resonance gives a measure of the lifetime of the corresponding quasibound state; thus the states corresponding to the sharper resonances require a longer coherence length in order to form. Correspondingly, the multipeak wave function at $E=4.063\,\mathrm{meV}$

[Fig. 2(c)] persists at this value of τ_ϕ, while the single peak wave function at $E=4.087$ meV [Fig. 2(b)] is washed out. To illustrate this, the corresponding wave function with phase breaking in the latter case is shown in Fig. 6(b). Note that the amplitude decays after the first dot. Interestingly, comparing Fig. 2(b) with Fig. 6(b), the patterns in the last two dots in the chain looks similar, while the pattern in the first dot, in particular, is considerably different. Thus it appears that the standing wave is only partially formed in this case. Despite the washing out effect, the bands and gaps are still present with the inelastic scattering. We note that a similar curve would be generated by introducing thermal broadening (this is done be convoluting G with the derivative of the Fermi function) and choosing $k_BT\sim\hbar/(2\tau_\phi)$. As one might expect given the above discussion, increasing the broadening by inelastic scattering or by finite temperature will cause the features to vanish in a progressive fashion. As shown in the inset, the resonant features are all smeared out by $\tau_\phi\sim 20$ ps ($l_\phi=\nu_F\tau_\phi\sim 1.4\,\mu$m). What remains is a series of larger peaks and dips that correspond to the positions of the bands and gaps. It is worth noting that the flat $G=1$ plateau, while no longer corresponding to exact quantization, appears to hold up quite well. This is because phase coherence in this case is much less of an issue. Specifically, with the skipping state shown in Fig. 2(e), the electrons only have to skip in and out of a dot only once and thus pass through rather quickly, in contrast with the comparatively long ''storage'' time it requires to form a scar.

With the Sinai billiard structure, we considered a single defect. We now consider a situation where the entire sample has some disorder. The middle thin curve in Fig. 6(a) now shows what happens when there are multiple defects in the original square dot structure at zero field. In this case, we have randomized the spacing of the fingers, so that there is a $\pm\delta$ variation of finger spacing off of an average of 0.31 μm, where δ is distributed between 0.00 and 0.01 μm. All other parameters, including the widths of the QPC openings are fixed. As one might expect, the $G=1$ plateau, which corresponded to the orbit skipping off the tops of the fingers [Fig. 2(e)], has vanished as a result of the disruption of the finger periodicity. What is also interesting here is that the conductance never exceeds one, despite the fact that we have not changed the width of the lead openings. Some remnants of the bands shown in the defect free curve are apparent, in particular, the group of resonances between 4.0 and 4.1 meV in Fig. 2(a) have an analog in the lower part of the defect curve, as does the $G=0$ gap at $E\sim 4.4$ meV. As one may expect, there is some shifting of the energy scale as dot size is no longer uniform. In the energy region between $E\sim 4.18$ and 4.32 meV, where $G=2$ and 1 plateaus are present in the clean system, the conductance remains close to zero in the disordered system. Importantly, unlike the perfect gaps in the uniform system, there are weak resonances superimposed on this $G=0$ ''plateau.'' Rather than a true band gap, this $G=0$ region is a by-product of the formation of localized states by the disorder. Introducing inelastic scattering with $\tau_\phi=100$ ps causes this plateau to be completely disrupted by the merging of broadened resonances (middle thick curve). For the bottom thin curve, we have also used similar variation of finger spacing, but with a different random configuration. The bottom thick curve has a phase breaking time of $\tau_\phi=100$ ps to be included. While the details of the curve are quite different from the previous example, the same qualitative behavior is evident—some remnants of bands and gaps survive, and the conductance does not exceed $G=1$.

Examples of resonant states in these disordered systems are shown in Figs. 6(c), 6(d), and 6(e). The wave function shown in Fig. 6(c) corresponds to the peak marked c in the middle thin curve ($E=4.4235$ meV here) and looks as if it holds an incompletely formed standing wave with two antinodes (note that the patterns in the third and sixth dots are almost identical). The second and third dots of wave function $d(E=4.4488\,\text{meV})$ contain a distorted version of the double dot ''molecular'' state shown in Fig. 1(e), while dots four, five, and six show a more irregular pattern. Wave function $e(E=4.28\,\text{meV})$ was obtained using the second impurity configuration. Here too is a distorted version of one of the double dot molecular states shown earlier. However, in this case it has the inverted-V pattern. As is evident to some extent in these pictures, the wave functions can become quite complicated when there is disorder, even in the case of resonant states. In some situations, it appears as if the wave function amplitude has percolated through the structure.

IV. CONCLUSIONS

In conclusion, in coupled dots, we find that resonances in conductance can occur as a by-product of the formation of molecular states that can be scarred by classical orbits that are shared between dots. In dot chains, we find that the states that contribute to the multiple resonance superlattice behavior can show scarring that can reflect complicated orbits that extend over many dots. In those cases, while the orbits in question are obviously related to the single and/or double dot orbits, they are clearly a nontrivial modification of them. Conductance plateaus can occur as a result of partially ''closed'' orbit states (as in Fig. 5), or from simple skipping orbit states (Fig. 2), the latter being present even without the application of a magnetic field. There are also cases where a plateau can not be easily identified with a particular orbit (Fig. 3). However, in general, with these well-defined multidot systems, we find that the quantum behavior largely reflects the underlying classical dynamics. The QPC's largely determine what orbits can participate and their role is in fact amplified in the case of multiple dots. It should be noted that collimation effect shown in Fig. 1(a) and the diamond scar shown in Fig. 1(b) persist even with a rounded potential.[8] We find that the same qualitative behavior occurs if rounded potentials are used but different multidot scars are possible depending on the degree of rounding. With regards to phase breaking and disorder, we find that the superlattice effects to be fairly robust to inelastic scattering, but rather sensitive to randomization of the dot periodicity.

It is difficult to see how these scarred states might be observed *directly* in a quantum dot system, but their occurrence should have important physical implications. For example, they should strongly influence any time-dependent excitation that involves the oscillation of charge between adjacent dots. As mentioned in the introduction, scarring has been observed directly in individual microwave cavities[4–6] and systems of coupled cavities have also been studied.[41]

The physics of ballistic quantum dots and microwave cavities is essentially identical, so direct observation of the effects we have shown may be possible in the latter system.

Finally, in closing, we mention that scarring in a periodically modulated quantum wire system was discussed, albeit briefly, by Luna-Acosta *et al.*[42] However, they considered relatively weak corrugations in contrast to the well-defined quantum dots examined here. As such, much of the discussion we have presented to explain our results (in particular, the analogy with ''atomic'' and ''molecular'' states in closed systems) is likely not relevant to their case.

ACKNOWLEDGMENTS

We acknowledge the financial support of ONR and DARPA and useful discussions with J. P. Bird.

[1] E. J. Heller, Phys. Rev. Lett. **53**, 1515 (1984).
[2] E. J. Heller, and S. Tomsovic, Phys. Today **46**(7), 38 (1993).
[3] E. J. Heller, P. W. O'Connor, and G. Gehlen, Phys. Scr. **40**, 354 (1989).
[4] S. Sridhar, Phys. Rev. Lett. **67**, 785 (1991).
[5] S. Sridhar, E. J. Heller, Phys. Rev. A **46**, R1728 (1992).
[6] A. Kudrolli, and S. Sridhar, Chaos **48**, 459 (1997).
[7] M. V. Berry and M. Tabor, Proc. R. Soc. London, Ser. A **356**, 375 (1977).
[8] R. Akis, D. K. Ferry, and J. P. Bird, Phys. Rev. B **54**, 17 705 (1996).
[9] R. Akis, D. K. Ferry, and J. P. Bird, Phys. Rev. Lett. **79**, 123 (1997).
[10] R. Akis and D. K. Ferry, Physica B **251**, 358 (1998).
[11] T. M. Fromhold, C. R. Tench, R. P. Taylor, A. P. Micholich, and R. Newbury, Physica B **251**, 334 (1998).
[12] J. P. Bird, D. K. Ferry, R. Akis, Y. Ochiai, K. Ishibashi, Y. Aoyagi, and T. Sugano, Europhys. Lett. **35**, 529 (1996).
[13] M. A. Kastner, Rev. Mod. Phys. **64**, 849 (1992).
[14] See C. Livermore, C. H. Crouch, R. M. Westervelt, K. L. Campman, and A. C. Gossard, Science **274**, 5291 (1996) and references therein.
[15] J. R. Barker and D. K. Ferry, Solid-State Electron. **23**, 531 (1980).
[16] J. Wang, Y. Wang and H. Guo, Appl. Phys. Lett. **65**, 1793 (1994).
[17] D. K. Ferry, R. Akis, D. P. Pivin, J. P. Bird, N. Holmberg, F. Badrieh, and D. Vasileska, Physica E **3**, 137 (1998).
[18] T. Usuki, M. Saito, M. Takatsu, R. A. Kiehl, and N. Yokoyama, Phys. Rev. B **52**, 8244 (1995).
[19] N. Berglund and H. Kunz, J. Stat. Phys. **83**, 81 (1996).
[20] R. Akis, J. P. Bird, and D. K. Ferry, J. Phys.: Condens. Matter **8**, L667 (1996).
[21] I. V. Zozoulenko, R. Shuster, K.-F. Berggren, and K. Esslin, Phys. Rev. B **55**, 10 209 (1997).
[22] L. Wirtz, J.-Z. Tang, and J. Burgdorfer, Phys. Rev. B **55**, 7589 (1997).
[23] L. Wirtz (private communication).
[24] M. Brack and R. K. Bhaduri, *Semiclassical Physics* (Addison-Wesley, Reading, MA, 1997), Sec. 2.7.
[25] E. B. Bogolmolny, Physica D **31**, 169 (1988).
[26] R. Akis, and D. K. Ferry, Semicond. Sci. Technol. **13**, A18 (1998).
[27] R. Akis, D. Vasileska, D. K. Ferry, and J. P. Bird, Jpn. J. Appl. Phys. (to be published)
[28] Z.-L. Ji, and K.-F. Berggren, Phys. Rev. B **45**, 6652 (1992).
[29] S. E. Ulloa, E. Castano and G. Kirczenow, Phys. Rev. B **41**, 12 350 (1990).
[30] D. W. L. Sprung, H. Wu, and J. Martorell, Am. J. Phys. **12**, 1118 (1993).
[31] M. Leng and C. S. Lent, Phys. Rev. Lett. **71**, 137 (1993); Phys. Rev. B **50**, 10 823 (1994).
[32] I. V. Zozoulenko, F. A. Maao, and E. H. Hauge, Phys. Rev. B **56**, 7975 (1996).
[33] F. Sols, M. Macucci, U. Ravaioli, and K. Hess, Appl. Phys. Lett. **61**, 1350 (1992).
[34] W. Porod, Z. Shao, and C. S. Lent, Appl. Phys. Lett. **61**, 1350 (1992).
[35] N. E. Hurt (unpublished).
[36] H. Wu, D. W. L. Sprung, J. Martorell, and S. Klarsfeld, Phys. Rev. B **44**, 6351 (1991).
[37] L. P. Kouwenhoven, F. W. J. Hekking, B. J. van Wees, C. J. P. M. Harmans, C. E. Timmering, and C. T. Foxon, Phys. Rev. Lett. **65**, 361 (1990).
[38] M. Buttiker, Phys. Rev. B **38**, 9374 (1988).
[39] G. Neofotistos, R. Lake, and S. Datta, Phys. Rev. B **43**, 2442 (1991).
[40] J. P. Bird, K. Ishibashi, D. K. Ferry, Y. Ochiai, Y. Aoyagi, and T. Sugano, Phys. Rev. B **51**, R18 037 (1995).
[41] A. Richter in *Emerging Applications of Number Theory*, edited by D. A. Hejhal, J. Friedman, M. C. Gutzwiller, and A. M. Odlyzko (Springer, New York, 1998), p. 479.
[42] G. A. Luna-Acosta, K. Na, L. E. Reichl, and A. Krokhin, Phys. Rev. E **53**, 3271 (1996).